Interface Adhesion and Reliability of Microsystem Packaging

Marvin I. Francis, Kellen Wadach, Satyajit Walwadkar and Junghyun Cho
Dept. of Mechanical and Materials Engineering, State University of New York, Binghamton, NY 13902-6000

ABSTRACT

Flip-chip technology is becoming one of the most promising packaging techniques for high performance packages. Solder balls are used as the connection technique in the flip-chip method and the connections are reinforced by filling in the spacing between the chip and substrate with underfill. The function of the underfill is to reduce the stresses in the solder joints caused by a coefficient of thermal expansion (CTE) mismatch. The presence of polymeric underfill material will, however, make the flip-chip packaging system susceptible to interfacial failure. Thus, the purpose of this study is to examine the interfacial delamination between the dissimilar materials in order to increase the reliability of the flip-chip interconnection method, and to understand the effect of underfill curing conditions on the interface adhesion. In particular, we use a linear elastic fracture mechanics (LEFM) approach to assess interfacial toughness. For this purpose, four-point bending testing is performed to determine a critical strain energy release rate, G_c. In addition, nano-indentation testing equipped with atomic force microscope (AFM) is employed to determine structure and properties of the underfill layer.

INTRODUCTION

Traditional packaging techniques are being replaced by the flip-chip/solder ball array packaging technique due to its increased input/output count, which increases performance [1]. The flip-chip interconnection system is a multilayer structure that is composed of a silicon die, solder balls, substrate, and underfill material. As a result, several interfaces are formed, including the silicon die/passivation, passivation/underfill, underfill/solder joint, underfill/solder mask, and solder mask/circuit board. The mechanical integrity of these different interfaces is, therefore, important in the reliability of the flip-chip package [2-5].

The interfaces that have proven to be a major source of delamination caused by a coefficient of thermal expansion (CTE) mismatch are the underfill/SiO_2 layer and the underfill/SiN_x passivation layer [4,5]. Underfill is composed of silica-filled epoxy resin, and fills in the spacing between the IC and the substrate, thereby minimizing the stresses on the solder joints. Delamination at these interfaces is caused by low fracture energy, which can lead to rapid fatigue crack growth into the solder joints.

Given that, we employ a reliable and repeatable LEFM based testing procedure that can be applied to examine the interfacial properties, particularly in flip-chip packages [6-10]. One objective of this research is to explore fundamental understanding on mechanical performance of the interfaces found in flip chip packages. This will be of greater importance when the packaging system becomes smaller as is the case for MEMS and MOEMS packaging.

For this purpose, a critical strain energy release rate, G_c will be measured as a function of varying interfacial conditions that result from underfill curing conditions. This can be used to identify specific curing conditions that may potentially have a negative effect on interface adhesion by comparing G_c's at these different conditions. These experiments will also be

supplemented by nano-indentation [11,12], atomic force microscopy (AFM), and scanning electron microscopy (SEM) in order to characterize the chemical and structural properties at the interfaces of the underfill.

EXPERIMENTAL PROCEDURE

Specimen Preparation

Two types of Si wafers were used in these experiments: silicon with a native oxide (SiO_2) layer and silicon coated with a nitride (SiN_x) passivation layer. A thin layer of underfill was dispensed onto the polished side of the rectangular specimen (≈30x45 mm^2). The silica-filled underfill epoxy resin was obtained from the Zymet Corporation (East Hanover, NJ). The underfill was allowed to spread uniformly over the specimen surfaces before another specimen was placed face to face, creating the sandwiched specimen. The sandwiched specimens were then cured in an oven using various curing parameters. After curing and cooling back to room temperature, specimens were diced into strips approximately 5mm wide by 45mm long using a diamond wafering blade. Finally, the pre-notch was made on the bottom silicon layer of the specimens.

Mechanical Testing

Interface fracture toughness testing was performed using a four-point bend test fixture that is attached to the mechanical tester (MTS858 Tabletop Testing System, Eden Prairie, MN) with a 100-N load cell. Sandwiched specimens (Si-beam/underfill/Si-beam) were placed in the four-point bend fixture and tested using 4-mm dia. loading pins. Tests were conducted using a displacement control at a constant displacement rate of 0.4 μm/sec. The load versus displacement data were obtained during testing, and the test was conducted at room temperature as well as at elevated temperatures.

The driving force that causes delamination can be expressed in terms of the strain energy release rate, G_c (J/m^2), provided that plasticity near the delamination area is limited [6]. The strain energy release rate becomes independent of delamination length and characteristic of steady-state growth as delamination propagates away from the pre-notch [6]. Applying these assumptions and using the beam theory yield G_c given by:

$$G_c = \frac{21(1-\nu^2)M^2}{4Eb^2h^3} \quad , \qquad (1)$$

where $M=PL/2$ is the bending moment, P is the load and L is the distance between loading pins. In addition, b is the beam width, h is the half thickness, E is the modulus of elasticity of the bulk substrate, and ν is the Poisson's ratio of the bulk substrate. The load P is taken from the load plateau of the load-displacement plot obtained from the interfacial adhesion test.

Nano-indentation test was performed to analyze and characterize the mechanical properties of the underfill material. This information can be of great value to better understand the interfacial adhesion. Testing was performed using a Nano-indentation System (Hysitron Triboscope, Minneapolis, MN), using a Berkovich shaped indenter tip. This instrument is equipped with an *in situ* imaging capability via AFM.

RESULTS

The critical strain energy release rate, G_c, was determined using the value taken from the load plateau of the load-displacement curve and Eq. (1). The interfacial adhesion tests at room temperature show that the interfacial toughness for the SiO_2/underfill interface is higher than that of the SiN_x/underfill interface. The average strain energy release rates for the SiO_2/underfill interface and for the SiN_x/underfill interface are 16.6 ± 1.4 J/m^2 and 6.6 ± 0.8 J/m^2, respectively (see Fig.1). The number of samples tested was four each, all of which were cured at 150˚C for 20 minutes.

The elevated temperature testing (at 140˚C) showed the same trend as that at room temperature while its magnitude was dropped by over two orders of magnitude. An average value of G_c for the former interface is 0.2 ± 0.07 J/m^2 and that for the latter interface is 0.03 ± 0.003 J/m^2. The number of samples tested was three each, all of which were cured at 150˚C for 20 minutes. This degradation is not unexpected considering that the glass transition temperature of the underfill material is close to 140˚C, resulting in extremely weak interfaces.

Nano-indentation testing was performed to compare the effect of curing conditions for the underfill materials. Our curing conditions are ranging from 150˚C to 170˚C at 10, 20, 30, and 40 minutes in air. As shown in Fig. 2a, the 150˚C cured specimens are softer (soft cure). It required at least 20 min to form a solid enough shape for testing. Further increase in curing time, however, makes the underfill degrade in hardness. As the underfill is cured at higher temperatures (e.g., 160˚C, 170˚C), hardness is increased significantly (hard cure), but again decreased after 20 min curing. Elastic modulus also displayed a similar behavior showing a maximum value at 20 min, followed by degradation in modulus in longer curing. This effect in modulus was still apparent at longer curing time (40 min) though a hardness decrease in the same period was not clear for the 170˚C cured specimens.

In fact, this behavior can be explained by the underfill settling as shown in AFM images after indentation (Fig. 3a and 3b), where longer curing time suggests less silica beads remained in the surface area, thereby resulting in lower surface hardness (i.e., larger indented area as shown in the figure). The 170˚C cured specimen that exhibited a similar drop in hardness and modulus did not show such a settling effect while still having larger silica beads on the surface for both 20 min and 40 min (Fig. 3c and 3d). It suggested that the curing at 170˚C be so fast that there was not enough time to flow the silica beads (particularly, larger beads) due to a rapid hardening of the underfill matrix.

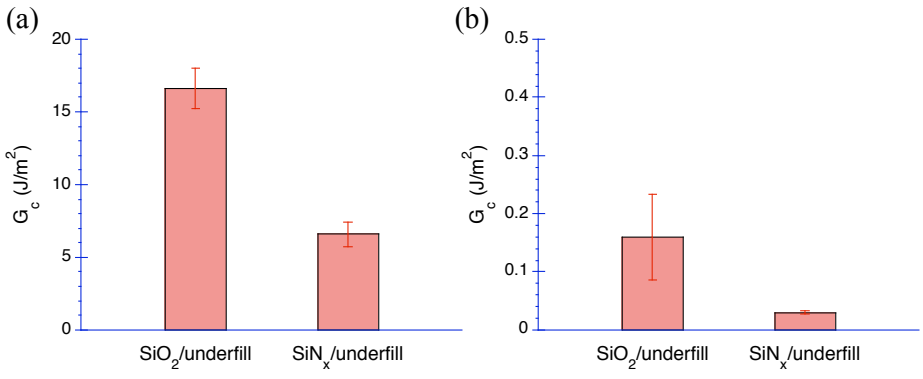

Figure 1: Interfacial fracture energy (G_c) for SiO_2/underfill interface and SiN_x/underfill interface tested: (a) at room temperature and (b) at 140°C.

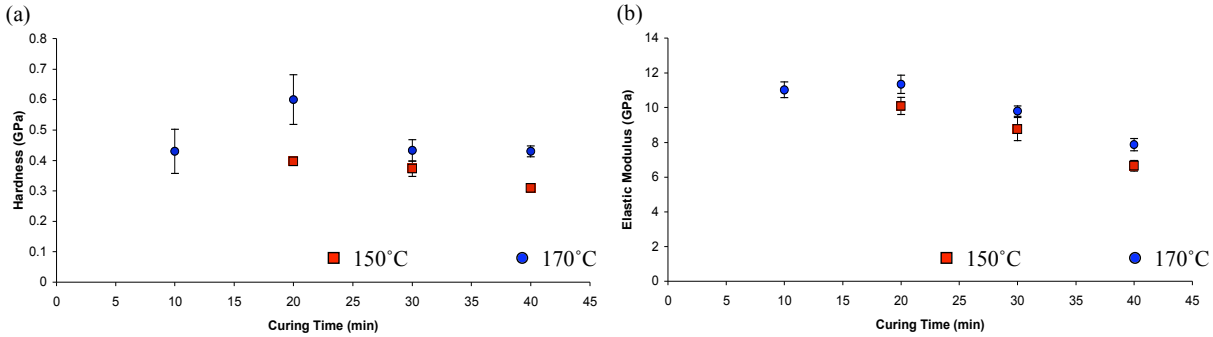

Figure 2. The plot shows the underfill properties vs. curing time for the 150 and 170˚C curing temperatures: (a) hardness; (b) elastic modulus. The data shown was obtained through nano-indentation testing.

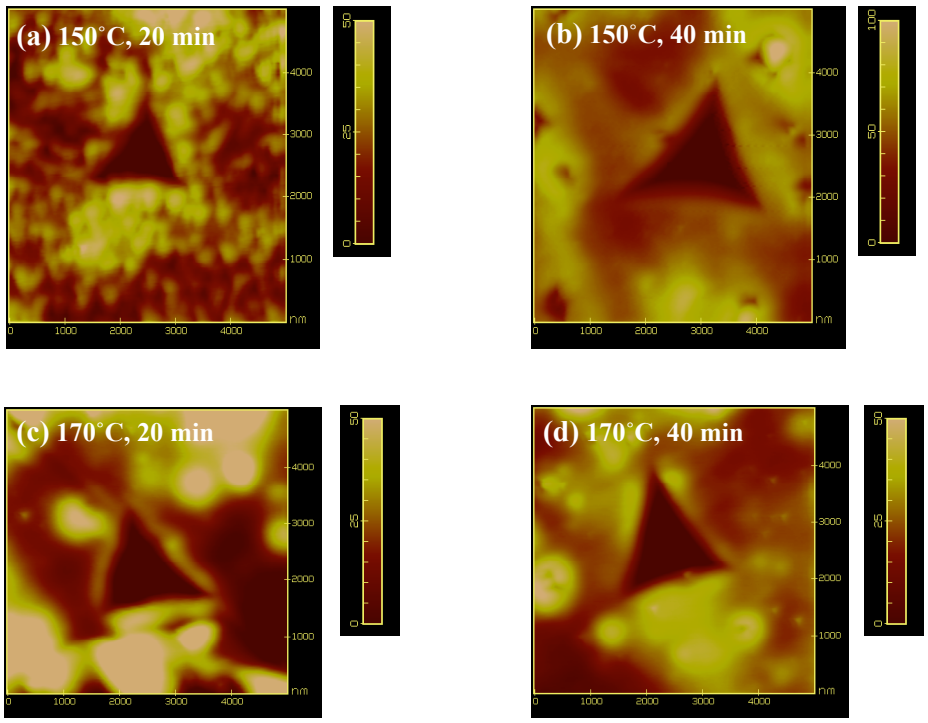

Figure 3. AFM images of the underfill materials after indentation: (a) cured at 150˚C, 20 min; (b) cured at 150˚C, 40 min; (c) cured at 170˚C, 20 min; (d) cured at 170˚C, 40 min. The triangular depressions shown in these images are from the Berkovich indenter tip, and round features in the surface images are from the silica beads. (Z-scale range is in nanometers)

In this regard, the underfill settling cannot be a sole reason for reduction in hardness and modulus. It may instead be attributed to the degradation of polymer chemistry at high curing temperatures, which results in a degradation of the underfill quality. Thermogravimetric analysis (TGA) on the above specimens is currently underway to have a fundamental understanding on this curing process.

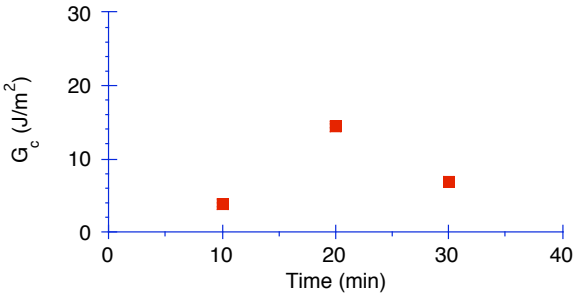

Figure 4. G_c values of the SiO_2/underfill cured at 170˚C at different curing time (tested at room temperature).

In fact, a similar drop in underfill properties is also observed in the interfacial adhesion test. As shown in Fig. 4, the interface fracture energy was a maximum value at 20 min, after which degradation was clearly visible. Each point represents for an average value of two specimens, and the difference was very small. The degradation behavior is indeed consistent with the above nanoindentation result.

AFM only shows the surface, so SEM analysis was used to view the cross section, and determine as to whether delamination occurs on the side with the smallest concentration of silica beads, or the side with the largest concentration of silica beads. Figure 5 shows that delamination indeed occurs at the interface with the finer and less concentration of silica beads. This indicates that underfill settling causes the interface with a small concentration of silica beads to be weaker, and that the larger and more silica beads may provide a resistance to interfacial delamination.

DISCUSSION

Based on our current results, there are two mechanisms that can explain the phenomenon of the mechanical properties of the underfill after the maximum values are obtained. One mechanism suggests that 'underfill settling' can cause the underfill to lose its particle strengthening at the location of less silica beads with increased cure times. Silica beads exist in a uniform configuration throughout the material before curing. Other studies have also shown that silica beads settle to the bottom of the underfill layer [7,8]. In this sense, flash curing at rather higher temperatures might prevent the settling effect, thereby retaining larger particles in the interfacial area.

The second mechanism suggests that the cross-linking structure of the underfill decomposes as the cure time increases. If it indeed occurs, it would not only decrease the materials properties, but it would also reduce the interface adhesion. As a result, choosing the right curing temperature and time is of utmost importance in the underfill performance by controlling the cross-linking structure and settling distribution of the underfill.

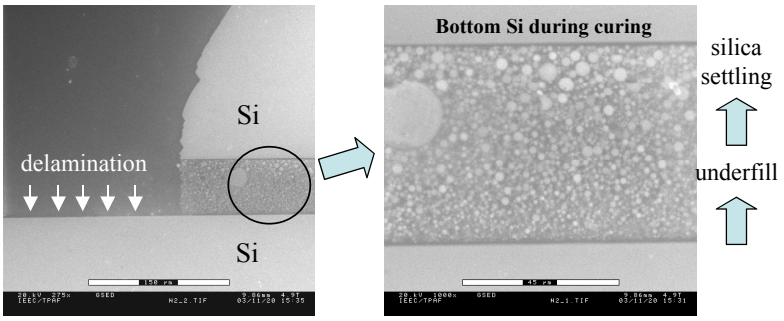

Figure 5. SEM images illustrating underfill settling: (a) cross sectional image of fractured four-point bend test specimen; (b) magnified view of (a) showing underfill settling.

At lower temperatures (150˚C), the underfill settling seems to be responsible for lower adhesion, while at higher temperatures (170˚C), the underfill chemistry seems to be important for the interfacial fracture energy. Further work needs to be conducted to confirm our results from the AFM, SEM, nanoindentation, and adhesion test of underfill settling. It is

therefore of great importance to establish the structure-property relation of the underfill by analyzing silica bead size, concentration, and distribution. In addition, TGA analysis will provide information on chemical properties/changes responsible for the degradation for longer curing time.

SUMMARY

Results characterizing the interfacial toughness of underfill used in flip-chip packages were analyzed and presented. G_c values for the SiO_2/underfill interface were ~16.6 J/m^2 and those for the nitride/underfill interface were ~6.6 J/m^2. As testing temperature increased to near glass transition temperature, both interfaces were dramatically degraded, but the SiO_2/underfill interface still displayed better adhesion than the nitride/underfill counterpart.

From nano-indentation and interfacial adhesion analysis, it is observed that the optimal cure times are 20 minutes for cure temperatures in the range of 150-170˚C. As the cure time increases, the values of hardness, elastic modulus and G_c all decrease. Underfill settling (esp. for larger silica beads) and polymer degradation can be the reasons for the sudden decrease in the properties of the underfill. More mechanical as well as chemical tests are underway to better understand the effect of underfill curing condition for enhanced interfacial properties.

ACKNOWLEDGEMENTS

This research was funded by the Integrated Electronics Engineering Center (IEEC) at SUNY Binghamton. MIF is currently supported by the Clark Fellowship at SUNY Binghamton. The authors would like to acknowledge the Zymet, Inc. for providing underfill materials. We would also like to thank Prof. R. Dauskardt for sharing some of his publications, and Dr. L. E. Felton for providing us with the nitride-passivated Si wafers.

REFERENCES

[1] H. Reichl, M. Shubert, and M. Tropper, *Microelectron Rel*., **40**, 1243-54 (2000).
[2] Z. Chen, B. Cottrell and W. T. Chen, *Surf. Interface Anal*., **28**, 146-49 (1999).
[3] C. E. Park, B. J. Han, and H. E. Bair, *Polymer*, **38** [15] 3811-18 (1997).
[4] S. Haque and G.-Q. Lu, *Microelectro. Rel*., **41**, 639-47 (2001).
[5] J. Wang, D. Zou, M. Lu, W. Ren, and S. Liu, *Eng. Fract. Mech*., **64**, 781-97 (1999).
[6] R.H. Dauskardt, M. Lane, Q. Ma, N. Krishna, *Engineering Fracture Mechanics*, **61**, 141-162 (1998).
[7] R.J. Hohlfelder, D.A. Maidenberg, R.H. Dauskardt, *J. Mater. Res*., **16**, 1 (2001).
[8] L. Wang and R.H. Dauskardt, Mat. Res. Soc. Symp. Proc., Vol. 682E, 1-6, 2002.
[9] A. A. Volinsky, N. R. Moody, and W. W. Gerberich, *Acta Mater*., **50**, 441-66 (2002).
[10] Q. Ma, *J. Mater. Res*., **12** [3] 840-45 (1997).
[11] M. F. Doerner and W. D. Nix, *J. Mater. Res*., **1**, 601 (1986).
[12] W. C. Oliver and G. M. Pharr, *J. Mater. Res*., **7** [6] 1564-83 (1992).